Hindawi
Advances in Meteorology
Volume 2022, Article ID 2179246, 17 pages
https://doi.org/10.1155/2022/2179246

Research Article

Local-Scale Weather Forecasts over a Complex Terrain in an Early Warning Framework: Performance Analysis for the Val d'Agri (Southern Italy) Case Study

Giuseppe Giunta,[1] **Alessandro Ceppi**,[2,3] **and Raffaele Salerno**[3,4]

[1]*Facilities Technical Authority Department, Eni S.p.A, San Donato Milanese, Milan, Italy*
[2]*Department of Civil and Environmental Engineering, Politecnico Di Milano, Milan, Italy*
[3]*Meteo Expert, Cinisello Balsamo, Milan, Italy*
[4]*University of Salento, Lecce, Italy*

Correspondence should be addressed to Alessandro Ceppi; alessandro.ceppi@polimi.it

Received 1 April 2022; Revised 17 September 2022; Accepted 29 September 2022; Published 19 October 2022

Academic Editor: Marina Baldi

Forecasting applications based on hourly meteorological predictions for weather variables are nowadays used in energy market operations, planning of gas and power supply, and renewable energy, among others. Available meteorological and climatological data, as well as critical thresholds of rainfall, may also have a key role in the hazard classification, related to slope instabilities of pipelines and critical infrastructures along routes. The present study concerns the performance of a weather forecast model in the framework of an early warning system (EWS) application, which supports the integrity management of oil and gas pipelines. This EWS has been applied on to a specific area: the Val d'Agri basin in the Basilicata region of Southern Italy, which is extensively affected by several landslides and floods. The hourly precipitation forecasts are provided by a dedicated meteorological model, the KALM-HD, using two different horizontal resolutions, 1.25 and 5 km, to analyze possible influences of the mesh grid size as well. On this area, several weather stations were specifically deployed to obtain observed data in a region where hydrogeological hazards are relevant for asset management. A comparison among observations and the KALM-HD scaled forecasts on six of these weather stations is presented to assess the model performance. Besides, precipitation, temperature, and wind speed are evaluated as well. The forecasting analysis is performed considering two years of data both on an overall and seasonal basis. Results show that the KALM-HD performs well with the 1.25 km grid, particularly on temperature and wind speed variables. Since weather stations can be gathered in two main sets depending on their positions, differences arise in the forecast quality of these two groups, related to orography and thermal effects, whose detection is difficult in the typical narrow valleys characterizing the area of study. This issue prevalently influences temperatures and local winds, which, these latter, are generally underestimated, while precipitation is mainly driven by synoptic circulation and its interaction with mesoscale meteorological features.

1. Introduction

In the framework of an early warning system (EWS) for water and pollution risk project, aimed to prevent and mitigate hydrogeological hazards along pipelines and strategic sites located along its routing, an application able to monitor and predict the degree of these dangers has been developed by the Eni company. It is well known that one of the most significant geohazards for onshore pipelines is related to landslides induced by ground movements [1, 2]. These phenomena are often caused by prolonged or intense rainfalls [3–5], and they can compromise the pipeline integrity (i.e., buckling, leaks, and structural failure) with associated economical loss due to service disruption, environmental pollution, and maintenance intervention [6–9]. In the period 1970–2019, a total of 1411 incidents were reported in the European gas transmission network (142,711 km), resulting in an annual primary failure

frequency of 2.9×10^{-4} per km [10], while in the period 2010–2019, the vast majority of "ground movements" was characterized by landslides.

Since this number is assumed to increase due to global changes [11, 12], in particular, to an intensification of extreme meteorological events [13, 14], landslide prediction at the regional scale is becoming a hot topic within the scientific community [15]. This calls for bigger efforts for the development of early warning procedures with the aim of issuing timely warnings of an upcoming hazardous event to temporarily reduce the exposure of vulnerable persons or infrastructure [16]. The forecasting of rainfall-triggered natural hazards with a rapid onset such as landslides and flash floods greatly benefits from numerical weather predictions (NWPs), especially from rainfall nowcasting and short-term forecasting that offer predictions several hours ahead [17]. Notwithstanding this, real forecasting initiatives, especially in the landslide community, are scarce [18, 19].

The EWS has been initially implemented in the Val d'Agri basin, an area of the Basilicata region in Southern Italy, to be further applied also on other Eni domains in Italy (e.g., the SecureGas project [20], in the framework of the European Horizon 2020 [21]). Using all available hydrogeological, geomorphological, and geotechnical data, the system defines critical thresholds of rainfall that can activate slope instability [22, 23], as well as a hazard classification of pipelines. In this context, rainfall meteorological forecasts are, therefore, essential to give a predicted view of possible hydrogeological-related hazards.

In this study, the NWP comes from a very high-resolution model, named KALM-HD, developed inside the framework of a more general forecast system (e-KMF®: eni-Kassandra Meteo Forecast, [24]). 60 hours of forecasted precipitation are entered into the EWS in advance and compared to precipitation thresholds related to possible rainfall-induced landslides. The exceeding of thresholds issues the generation of a warning in any segment of the pipeline network, useful for asset integrity management and the prevention or mitigation of related hazards.

In this framework, it is evident that the precipitation forecast plays a crucial role in the proposed EWS: therefore, a benchmark analysis to assess the performance of weather forecast generated by the KALM-HD meteorological model is required before being fully operational and described here as the scope of the work.

The study presents the main results for an observation period of two years between December 1st, 2018, and November 30th, 2020, about measured meteorological variables compared to weather forecasts provided by the KALM-HD model, evaluating data both on the overall period and seasonal basis without any calibration nor data filtering. This benchmark analysis is conducted for temperature, precipitation, and wind forecasts, by matching data coming from six weather stations placed in the Val d'Agri area. Skill scores of performances are used to understand the reliability of these weather forecasts at the lead time day +1, considering the first 12–36 hours of the forecast horizon, since the model is daily initialized at 12 UTC. This warning time is enough to allow an intervention to mitigate or avoid possible structural failures induced by ground movements due to significant rainfall. The statistical analysis has been evaluated using the model data at two horizontal resolutions, 1.25 and 5 km, so that the forecasted meteorological variables were scaled on the same points where the weather stations are placed.

Figure 1: The application case study is in the Val d'Agri, Basilicata, Southern Italy. The blue placemarks identify the seven operational weather stations specifically installed in the region. Over six of them, a benchmark analysis for short-term temperature forecasts has been carried out.

The structure of the paper is as follows: Section 2 describes the area of study which is the Val d'Agri catchment in the Basilicata region in the south of Italy, a complex, prevalently mountainous, territory in the Mediterranean basin, highly subjected to hydrological and geological risk such as floods and landslides. Section 3 highlights the implemented KALM-HD meteorological model with its main features and setup schemes and the observed measurements coming from the six weather stations installed in the southern Apennine region. The main results and discussion about the performance of the meteorological model in comparison with the observed data are illustrated in Section 4 with a detailed analysis of temperature, precipitation, and wind variables.

2. Area of the Study

2.1. The Val d'Agri Area, Basilicata Region (Southern Italy). The Basilicata region is placed in the south of the Italian peninsula with two accesses to the sea (Figure 1): the Tyrrhenian on the west and the Ionian on the east. This geographical situation influences its climate. On one side, there is the continental element, which dominates the high pressure, determining hot dry summers and severe dry winters; on the other side, the Mediterranean sea influences the Basilicata west coast with humid weather in almost all seasons. As a whole, the sequence of seasons resembles a very irregular succession of cyclones and anticyclones, explaining a sort of its unpredictability and strong weather contrasts over the years. Thus, all districts in this region are affected by this meteorological instability.

Moreover, Basilicata is experiencing a growing number of multiday extreme weather situations [25] and, it is also known for the highest frequency of extreme hydrological and geological events [26]. For these reasons, it is one of the

Table 1: Geographical positions and altitudes of the six weather stations installed in the Val d'Agri area and used in the analysis of the model performance.

n.	Weather station	Location	GPS coordinates		Altitude (m)
1	Area Pozzo, Agri 1	Marsico Nuovo, Loc. Campo Reale	40°25′43″N	15°44′53″E	840
2	Area Pozzo, Cerro Falcone 2	Calvello, Loc. Bosco Auterio	40°26′13″N	15°47′59″E	1330
3	Area Pozzo, ALLI4, Monte ENOC 10	Viggiano, Loc. Masseria Cascia	40°22′52″N	15°52′39″E	1290
4	Area Pozzo, Costa Molina 2	Montemurro, C.da Costa Molina	40°19′31″N	15°59′21″E	1040
5	Area Eni Cova	Viggiano	40°19′11″N	15°54′13″E	880
6	Area Pozzo, Innesto 2	Marsico Nuovo, C.da Spineto	40°21′47″N	15°47′08″E	600

Italian regions most prone to hydrogeological hazard, in which nearly 50% of the towns are classified as exposed at high risk of landslides or floods [27–29], due to its geological characteristics and dynamics of precipitation, which produce extensive damages to regional urban areas and infrastructures [30]. From historical analyses [31], it is emerged that about 80% of the considered events occur after precipitation with a duration from 1 to 6 days of which about 60% is between 2 and 3 days, with a range of average precipitation intensity between 0.5 mm/h and 3.5 mm/h; the remaining 20% concerns events lasting up to 15 days. Furthermore, about 60% of the landslides were triggered by rain events with return periods of less than 5 years (in particular, more than 30% of them have less than 2 years), while events with a return period greater than 20 years represent about 25%.

In this context, the Val d'Agri area matches all the mentioned characteristics in terms of hydrological and geological hazards in accordance with other studies in the Mediterranean basin [32, 33]. Numerous active landslides are present in this territory, and the above-cited past analyses also demonstrate the importance of observations to measure the rainfall intensity and duration. For this reason, further weather stations have been installed over this area of study to collect data where other near-surface measurements are less available. These measurements are compared to temperature, precipitation, and wind forecasts, daily produced by the KALM-HD model.

3. Materials and Methods

A project aimed to implement an early warning system (EWS) for geohazards has been developed by the ENI company, following the need to support the integrity management of oil and gas pipelines and to plan and manage possible criticalities along the assets in a region strongly affected by several hydrological and geological facts. The EWS is capable of forecasting potential hydrological and geological risks related to natural events (e.g., flooding and slope instability) with a particular focus on possible landslides, triggered or reactivated by local weather occurrences. In this context, meteorological observations and forecasts turn out to be fundamental components of data integration in the implemented system as shown in Figure 2.

However, to ensure high reliability of weather forecasts in the implemented EWS, a deep analysis is necessary to assess its performance before being fully active. Comparisons between weather station data and the KALM-HD meteorological forecasts for temperature, precipitation, and wind have been executed between December 1st, 2018, and November 30th, 2020. As proposed by Giunta et al., [34], in order to calculate the model performance, common skill scores from the scientific literature are used: the mean error (ME), the mean absolute error (MAE), the root mean square error (RMSE), the determination coefficient R^2, and the Nash-Sutcliffe (NS) index [35–37].

Values have been scaled to the points where weather stations are installed, but no calibrations nor filters [38] have been used in this comparison since the aim is to verify the performance of the model itself without any post-processing correction algorithm. Two years of data can give a good test evaluation across different seasons and weather patterns, although general conclusions cannot be drawn about the KALM-HD uncertainties and their impacts on the EWS, since only a small percentage of severe events has occurred in these analyzed years. Lastly, possible biases to be corrected are highlighted and analyzed considering both the two different horizontal resolutions at 1.25 and 5 km of the KALM-HD model.

3.1. The KALM-HD Meteorological Model. In the framework of the e-KMF® project, originally built for making weather predictions from short-term to seasonal scale [24–39], a LEPS (limited-area ensemble prediction system) has been developed and implemented a few years ago. This system benefits from the initial and boundary conditions from the global scale ensemble prediction produced by e-KMF®. The LEPS methodology allows combining the benefits of the probabilistic approach with the high-resolution detail of a limited-area model (LAM), and a better representation of local characteristics has a key role in a good prediction of all near-surface parameters. This LEPS, together with its uncertainty issues, gave rise to an application, named KALM (Kassandra ALpine Model), used in the Alps area at 3 km as horizontal resolution.

This original model was further developed for local areas, and a new improved version, the KALM-HD (high definition) at a 1.25 km resolution, has been inserted in the geohazard application for the Val d'Agri case study. Computation on a larger domain at 5 km as horizontal resolution provides boundary conditions to the inner model at 1.25 km, and, in this study, it has been also assessed in comparison with observations to better understand the effects of the mesh grid size (Figure 3) in an area characterized

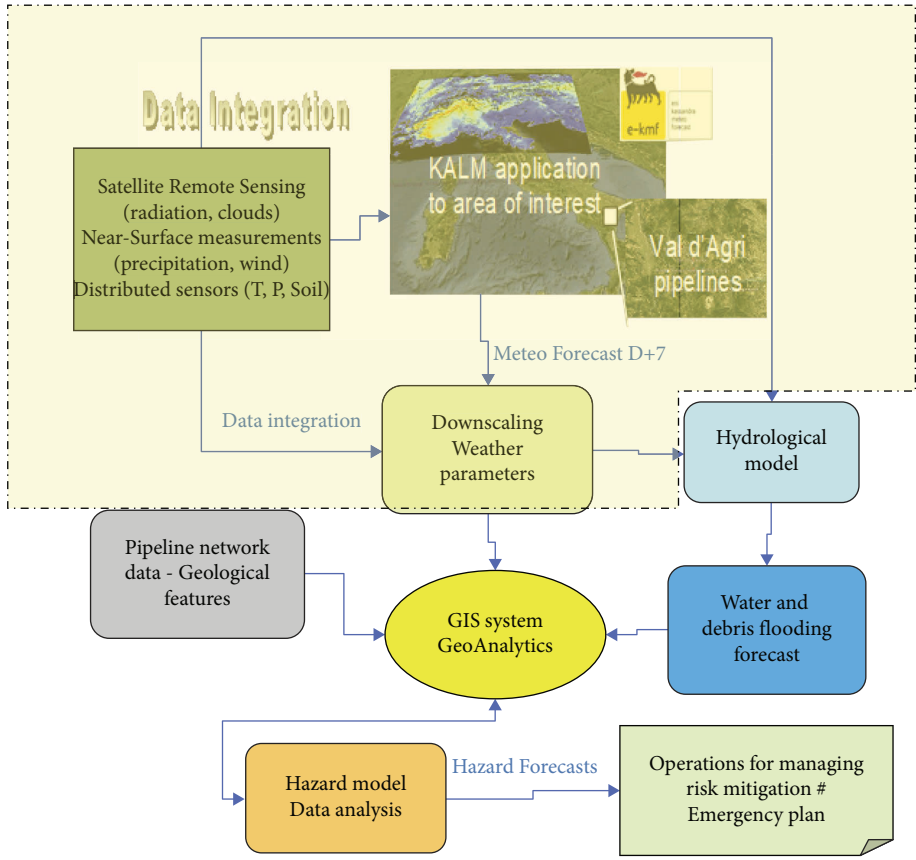

Figure 2: The early warning system workflow diagram. The light-yellow box highlights meteorological components as data integration in the project.

by a complex orography, narrow valleys, and strong thermal-dynamical effects.

During that development, PBL (planetary boundary layer) schemes, land-surface processes, treatment of orography, and choices of physical schemes in the KALM-HD model have been deeply revised, showing their importance in those mountainous areas at such horizontal resolutions. The ensemble spread, which is also a significant issue, due to the limited number of members used, has to be considered with the linkage of the traditional downscaling mechanism. Concerning this aspect, a dynamical downscaling approach has been adopted for the KALM-HD. However, the knowledge of local characteristics and the definition of observed data were important. This latter can be used to define dynamics and thermodynamics in the local domain and to get a reasonable predictability horizon, which is usually reduced with an increased resolution. Moreover, the effects of interaction between synoptic circulation and mesoscale may be remarkable on all atmospheric variables and, particularly, to the near-surface ones in an area where topographic features are relevant to the small-scale fluxes.

3.1.1. The KALM-HD Ensemble Prediction Model. As cited above, the local ensemble prediction system (LEPS) methodology used by the KALM-HD model is based on the idea of reducing the number of LAM needed integrations by an order of magnitude, retaining a large amount of the global ensemble information, and decreasing the number of ensemble elements subjected to LAM runs. The modeling chain starts with the e-KMF® global forecast system, which uses the same multimodel and ensemble technique as in [24], but with a horizontal resolution of 0.5°; therefore, outputs of the whole ensemble system have the same regularly spaced latitude-longitude grid. Each member is initialized by the corresponding initial conditions of the 20 members of the GEFS (global ensemble forecast system) by the NCEP (National Center for Environmental Prediction). The number of 40 members of the obtained ensemble can be doubled using a time-lagged technique with the two data runs at 00 and 12 UTC, obtaining a total of 80 members. Computational considerations motivate the use of forecasts based on lagged ensembles, whereby forecasts initialized at different starting dates, but verified on the same target date, are averaged. The next step is grouping the global ensemble members into several clusters and then choosing a representative member (RM) within each one. Every RM is representative of the possible evolution scenario associated with each cluster which provides both initial and boundary conditions for a high-resolution LAM integration. The following step is the intermediate computation by the KALM-HD model on a centered domain at 5 km as a horizontal resolution on Italy to provide boundary conditions to the inner model at 1.25 km. At this step, no data

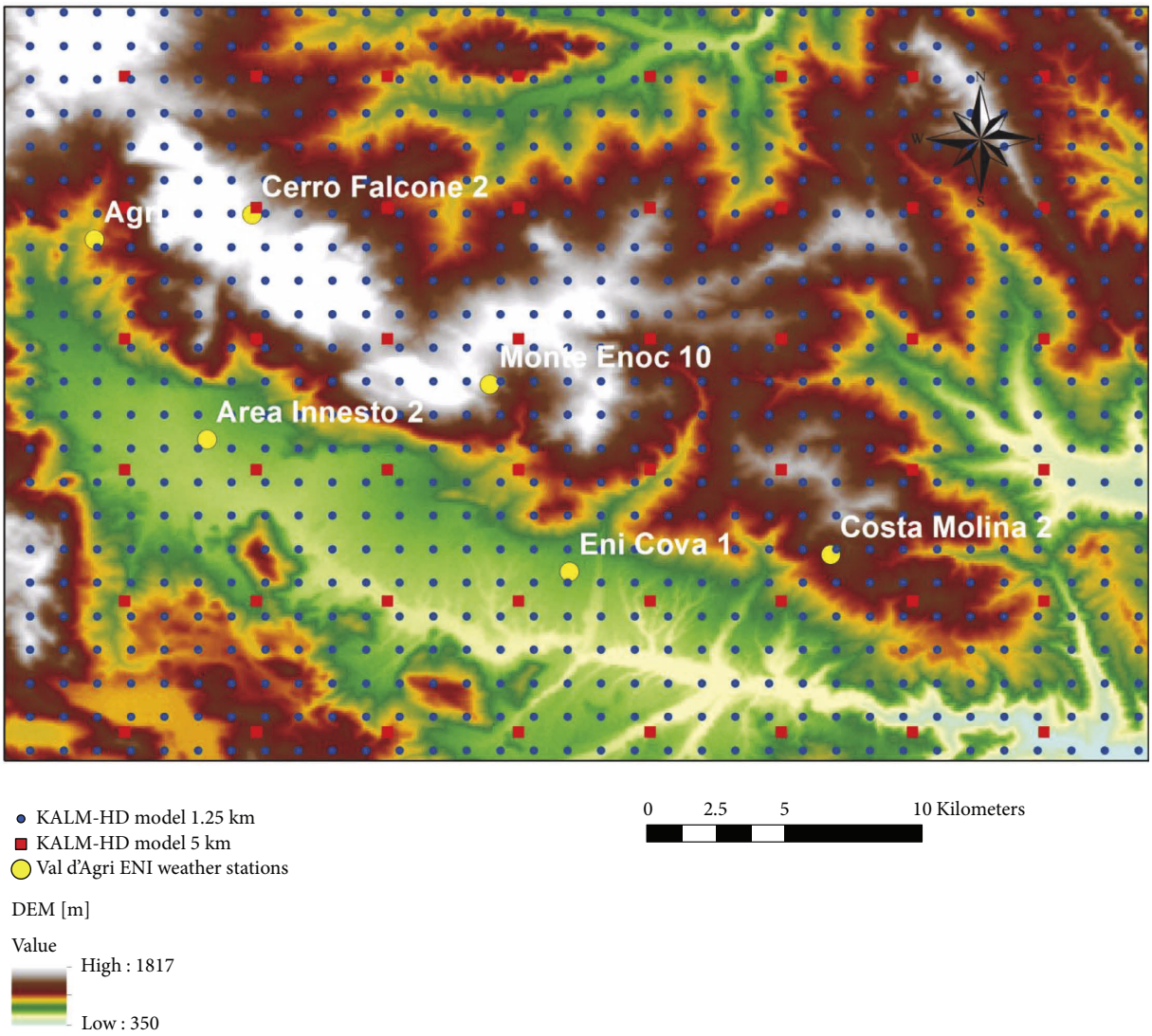

FIGURE 3: The two horizontal grid resolutions of the meteorological model KALM-HD at 1.25 km (blue dots) and 5 km (red squares). The six weather stations (yellow dots) used in the benchmark analysis are represented in the figure as well.

assimilation is carried out to reduce computational costs. Finally, the KALM-HD model is ready to compute forecasts on the Basilicata region and over the Val d'Agri area at 1.25 km as horizontal resolution.

Since precipitation is the main driving variable for any hydrogeological application; its definition in terms of localization and intensity is very crucial for the local-scale application made by the KALM-HD in Val d'Agri; hence, the model at 1.25 km makes forecast up to 60 hours. This is because in such a complex topography and at a resolution comparable to the convective scale, predictability may be quite short. However, it is true that increasing horizontal grid resolutions into the convective-allowing regime may lead to significant improvements in convective forecast guidance, especially in this area.

3.2. Data Assimilation Process. All available measurements should be used in the KALM-HD model data assimilation, which provides an objective methodology to combine observational and model information, giving an estimate of the most likely atmospheric state and its uncertainty. This approach adds value to the observations, by filling in the space-time gaps to observations, and the model, by constraining it with the measurements [40]. Moreover, local station data can be also used to calibrate forecasts at those points. Surface observations (2 m air temperature and relative humidity, winds, and pressure) may have relatively good spatial (a few kilometers) and time resolution (one hour or less), but their use in atmospheric data assimilation has proven to be substantially difficult. In the KALM-HD, an ensemble Kalman Filter (EnKF, [41]) scheme has been applied, which extracts dynamical information directly from the forecast model, and it produces analysis increments that depend on the local state of the PBL and its recent history. The main advantages of the EnKF provide an estimate of the forecast and analysis error covariances, and that is much simpler to implement than 4D-Var. The EnKF can be viewed as an

Figure 4: The six weather stations installed in the Val d'Agri basin by the Eni company.

approximate version of the Kalman Filter, in which the state distribution is represented by a sample or "ensemble" from the distribution itself. This ensemble is, then, propagated forward through time and updated when new data become available. The ensemble representation is a form of dimension reduction, which leads to computational feasibility even for very high-dimensional systems. In the EnKF, the relative weighting in the analysis between the background and observations, and the influence of observations away from the station locations, are determined by anisotropic and inhomogeneous background covariances. These covariances, in turn, are estimated from the ensemble itself of the short-range forecasts, using the full nonlinear model, and the covariances will, therefore, change as the PBL evolves, as shown by Hacker and Snyder [42] using a single-column model, and Fujita [43] assimilating actual surface observations in the EnKF. In addition, to examine the role of forecast model error, they demonstrated important improvements in the analysis of mesoscale features for two severe weather cases as well as improvements lasting 6–12 h in the subsequent forecasts. Meng and Zhang [44] briefly examined the assimilation of surface observations in a case study of a mesoscale convective vortex, but they found little influence on the short-range forecast. The effectiveness of the EnKF in the assimilation of surface observations and the improvements of the following forecasts in the boundary layer and further aloft as well as at the surface, has been confirmed by several studies [45]. Surface pressure observations reflect the distribution of mass vertically integrated through the depth of the entire atmosphere, and their use in the EnKF has been explored by Dirren [46] and Compo [47], for example. The assimilation of surface pressure should improve the forecast in terms of a better dynamical representation, which, in turn, can influence all other parameters.

The EnKF in the KALM-HD has then been based on the above-cited studies to develop the model data assimilation. However, the implemented system in this study largely ignores forecast model errors, despite their potential importance in the PBL and, therefore, in the assimilation of surface observations. In fact, in the present paper, the system only includes a spatially and temporally varying, adaptive inflation [48], which compensates for underestimation of the analysis variance by the EnKF as well as under dispersion in the ensemble forecasts owing to un-represented model error. There are other possible approaches specifically aimed at representing model uncertainties within the EnKF, employing multiple suites of physical parameterizations [43–49] and including an additive noise or "backscatter" scheme within the model [50]. These approaches may be analyzed in the future evolution of the model data assimilation.

3.3. Local Weather Measurements. Six weather stations, shown in Table 1 and Figure 4, were installed between June and August 2018, while a seventh was mounted a year later,

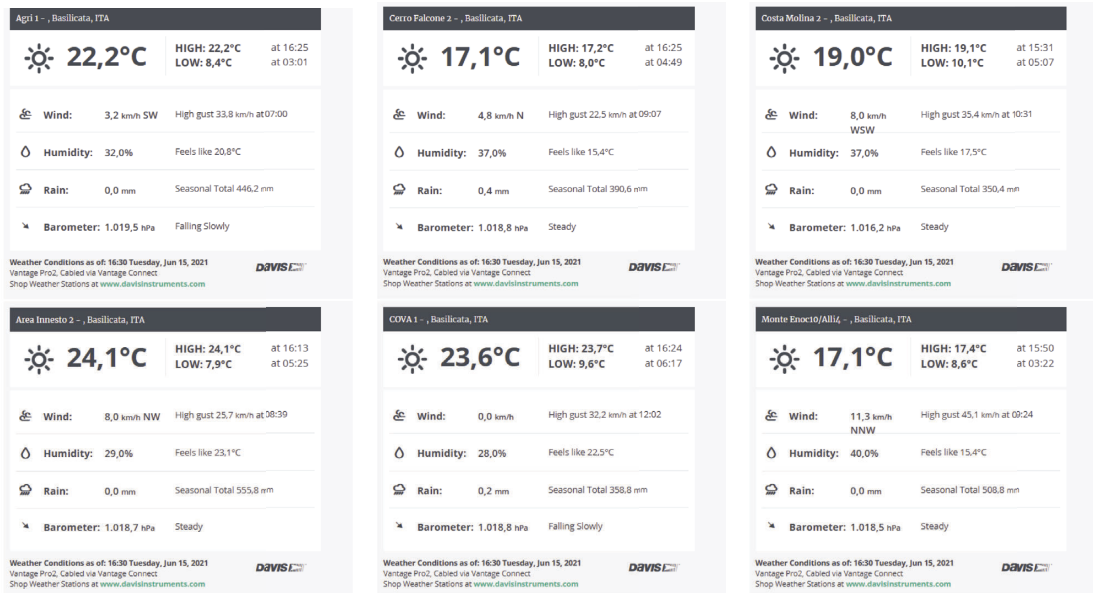

Figure 5: An overview of the real time monitoring control for the six weather stations in the Val d'Agri catchment.

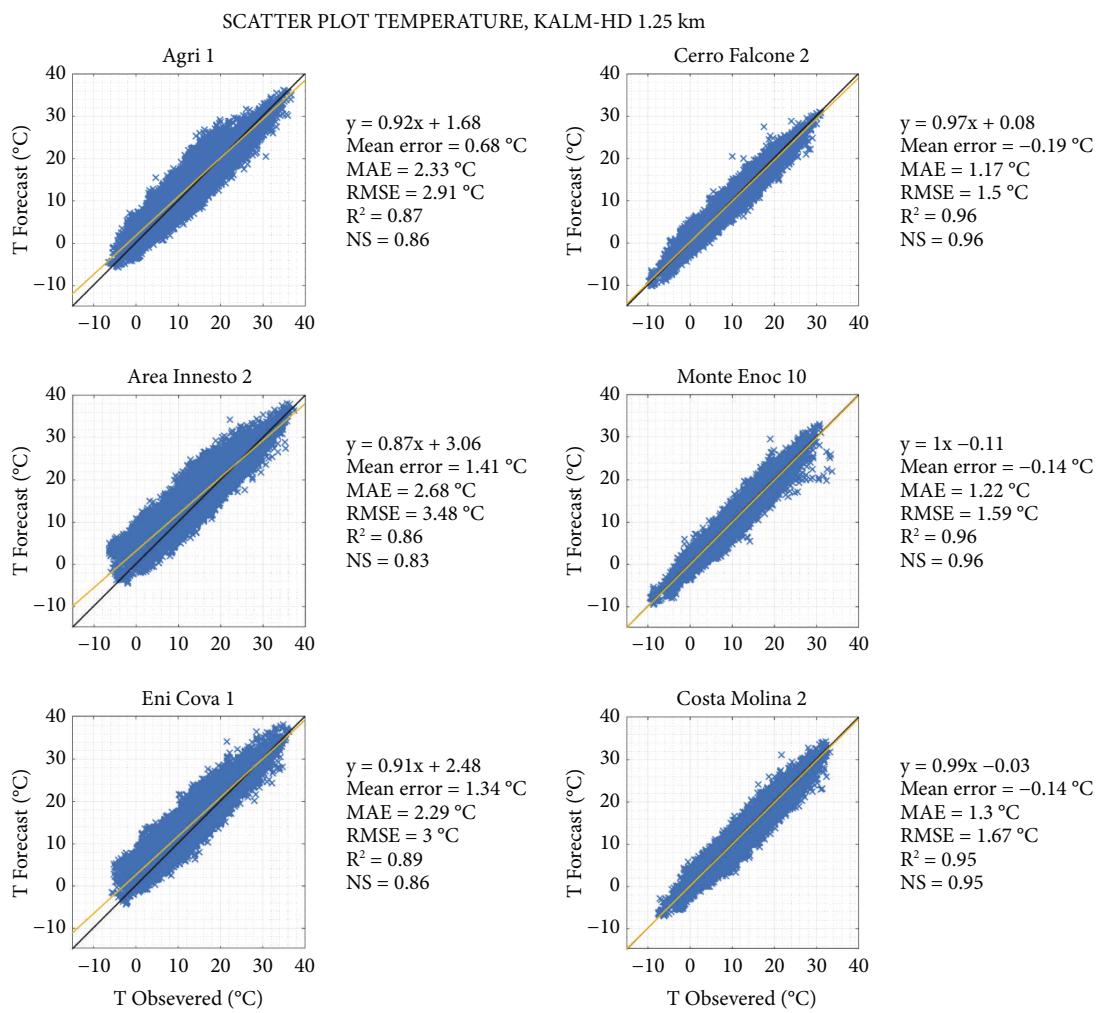

Figure 6: Scatter plots of the KALM-HD model with 1.25 km as grid resolution vs. observed data for the hourly temperature forecast over the six stations at day +1 as lead time for the whole two years of the observation period. On the left are the "valley stations," and on the right are the "mountain stations."

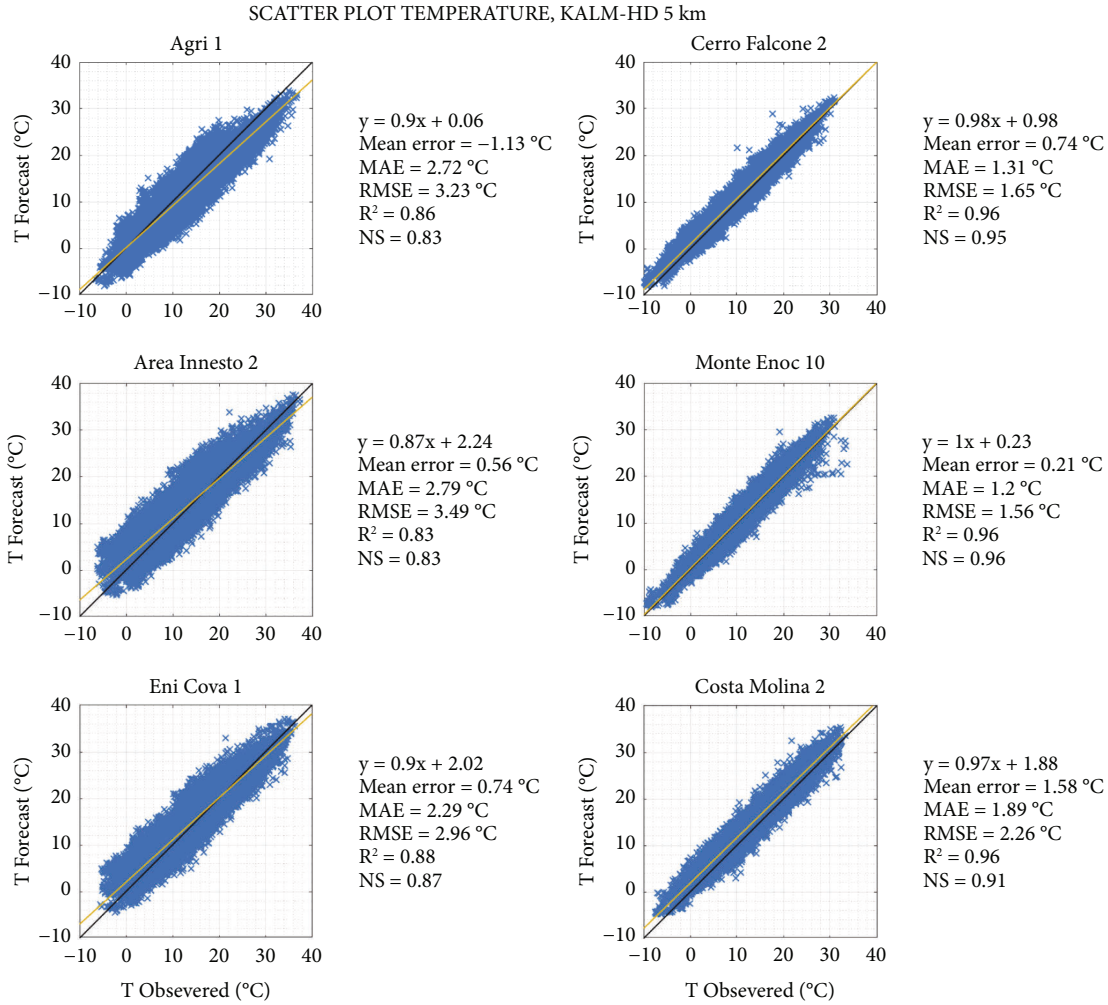

Figure 7: Scatter plots of the KALM-HD model with 5 km as grid resolution vs. observed data for the hourly temperature forecast over the six stations at day +1 as lead time for the whole two years of the observation period. On the left are the "valley stations," and on the right are the "mountain stations."

in November 2019. For this reason, the comparison between observed and forecasted data has been carried out only with the first six, covering a period of two years as an available dataset. Observed temperature and wind data are discussed with forecasts on an hourly basis, while precipitations are aggregated on a daily scale. The performance analysis carried out at lead time day +1 covers the first 12–36 hours out of 60 of the whole forecast horizons, as the model run is daily initialized at 12 UTC.

All the weather stations are under regular maintenance and control service by the Eni staff and by the authors themselves. However, some technical problems occurred during these two years of dataset, hence, missing days are omitted in this analysis; this also explains why the total percentages of analyzed events regarding precipitation and wind plots are not 100%, since the remaining difference is attributed to those days and hours with no available data which were conveniently filtered out.

All installed weather stations (Figure 4) are Davis Vantage Pro 2 of modern technology, which allow the real-time acquisition of main meteorological variables: air temperature and relative humidity, atmospheric pressure, precipitation, wind speed, and direction, and further derived parameters such as the heat index, wind chill, and dew point. Through a GPRS modem connection, transmitted data can be consulted by all operators of the EWS project who can check in real time local weather and environmental conditions (Figure 5) and make all proper actions and decisions for management and planning of the territory.

4. Results and Discussion

The following analyses show the comparison between the KALM-HD model forecast, using the two available horizontal resolutions at 1.25 km and 5 km, respectively, and the observed weather data by the six weather stations located in Val d'Agri for an overall two-year period, from December 1st, 2018, to November 30th, 2020, and for each season. Due to their positions near the bottom of the valleys and near the edge of the mountains, weather stations are divided into two categories: "valley stations" (Agri 1, Area Innesto 2, and Eni Cova) and "mountain stations" (Cerro Falcone 2, Monte

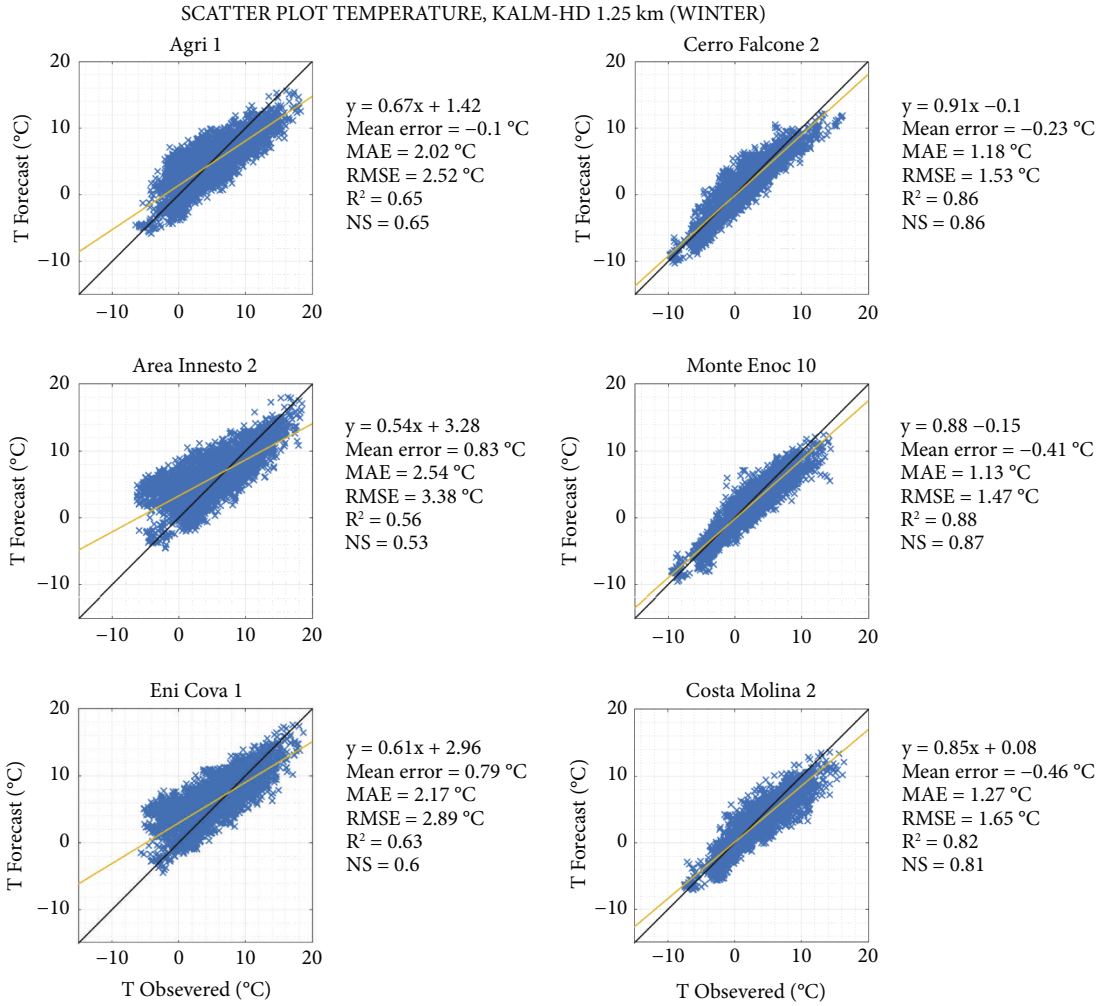

Figure 8: Scatter plots of the KALM-HD model with 1.25 km as grid resolution vs. observed data for the hourly temperature forecast in winter (DJF), over the six stations at day +1 as lead time for the whole two years of the observation period. On the left are the "valley stations," and on the right are the "mountain stations."

Enoc 10, and Costa Molina 2). Therefore, the following results are consequently displayed when referring to these two classes. An analysis of seasonal characteristics has also been carried out to look at possible differences linked to each three-month period of winter (DJF), spring (MAM), summer (JJA), and autumn (SON) included in the observation period.

It is worthwhile to remember that the conducted analysis evaluates the performance of the KALM-HD raw values, using both the horizontal resolutions without any post-processing of the model output nor calibration at the forecast point.

4.1. The KALM-HD Comparison between Forecasts and Observations

4.1.1. Temperature Analysis. Regarding temperatures, results show a better performance for the higher resolution model over all six weather stations, in terms of ME, MAE, RMSE, R^2, and NS index. A significant outcome is the better performance found over the three mountain stations in comparison with the valley ones. In fact, the determination coefficient is about 0.96 for those located at the top of the hills, while for the others on the valley floor is between 0.83 and 0.89 considering the two grid resolutions. The same outcome is observed for the NS index which is above 0.80 and 0.90 for valley and mountain stations, respectively. As far as concerning the MAE, this is generally between 1.17°C and 1.89°C for the mountain stations, while it is between 2.29°C and 2.79°C for the valley ones. This latter score could certainly be improved since an acceptable threshold of 2°C is set as focal target in temperature prediction [34]. However, this flaw can mainly be explained by the pronounced orography present in the Val d'Agri area (see Figure 3). In fact, sites located at the bottom of valleys are generally affected by those phenomena of complex terrain, typically at mesoscale α or β [51], such as thermal inversion during nights, subsidence, and katabatic effects due to local wind circulation, which are difficult to be properly foreseen even by a weather model at such a resolution of 1.25 km. As it is shown in Figures 6 and 7, the meteorological model has the

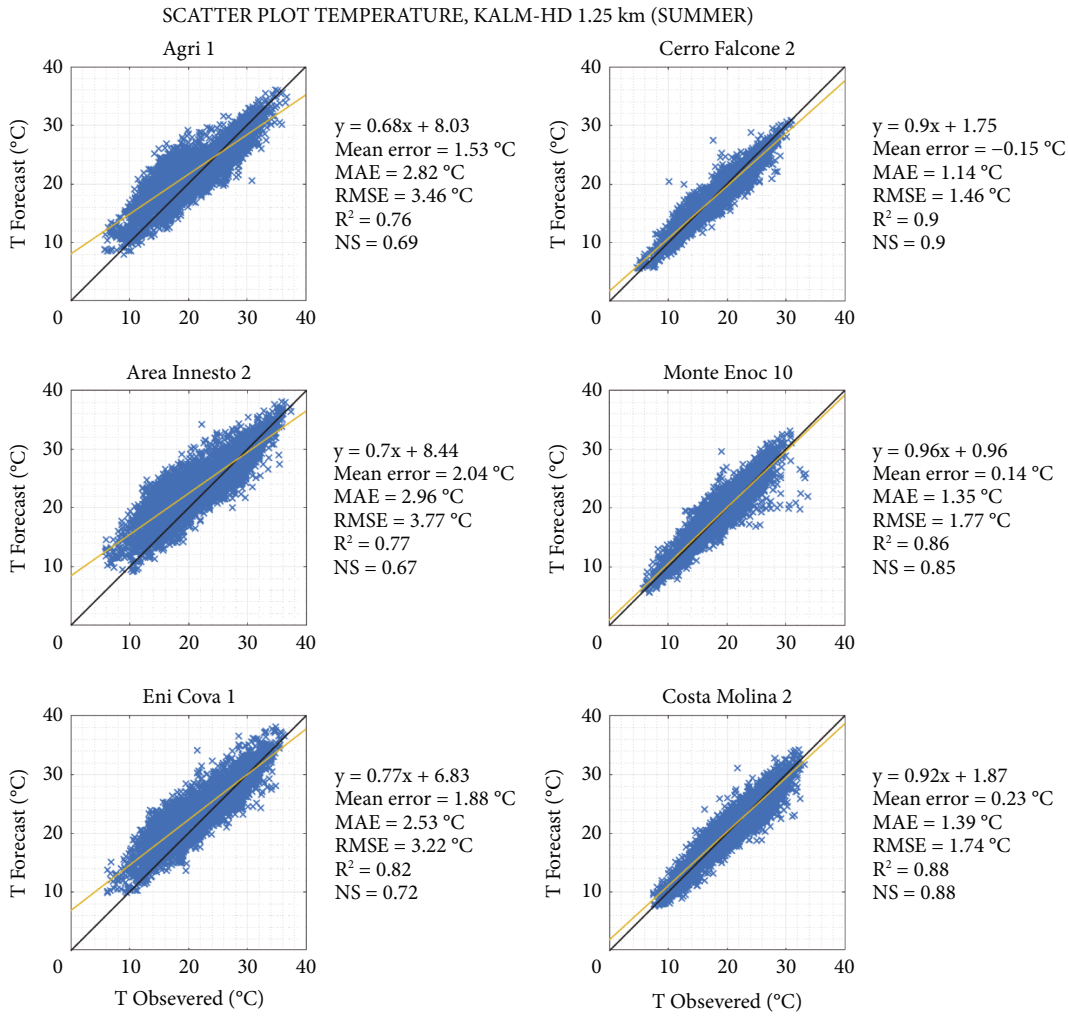

Figure 9: Scatter plots of the KALM-HD model with 1.25 km as grid resolution vs. observed data for the hourly temperature forecast in summer (JJA), over the six stations at day +1 as lead time for the whole two years of the observation period. On the left are the "valley stations," and on the right are the "mountain stations."

tendency to overestimate low temperatures (especially during cold months) over the valley stations, in comparison with the mountain ones, where temperature values are mostly affected by the interaction of synoptic patterns, which are generally more predictable. Notwithstanding this, it is relevant to remark that all skill scores obtained by the KALM-HD model with the two grid resolutions are reasonably satisfactory during these two years of comparisons, especially over mountain sites.

Concerning the seasonal behavior, wintertime forecast errors are greater than in the other seasons in the valley stations, and emphasizing the unresolved thermal inversion effects (Figures 8 and 9).

In winter, local subsidence plays an important role in fair weather conditions and, due to the geographical conformation of the area, the daytime breakup of the temperature inversion is more difficult. It is well-known that valleys produce their own local wind systems as a result of thermal differences [52]. The most developed and symmetric wind system might be anticipated in a deep, straight valley with a north-south axis. Some asymmetries may develop with time due to the diurnal variation of the solar radiation input to west- and east-facing slopes. In this case, the main valley near the measurement points is mostly east-west oriented with a sensible difference in terms of solar radiation along seasons. In the case of sunlight, larger-scale winds, up-valley, and upslope, usually form during the day due to surface heating. At night, surface cooling commonly leads to drainage flows in the reverse direction. This representation may be also influenced by the presence of small orthogonal valleys which may interact with the cross-valley wind component linked to the differential solar heating of the valley slopes.

In nocturnal situations, the coldest (and densest) air settles down to the lowest level, and, therefore, the potential temperature increases with height above the valley floor. Over this stably stratified layer of the atmosphere, the normal adiabatic decrease of temperature with height usually prevails. For all these considerations, mountain stations do not show significant differences in all seasons.

Due to these topographic-induced characteristics and some model limitations to reproducing narrow valley

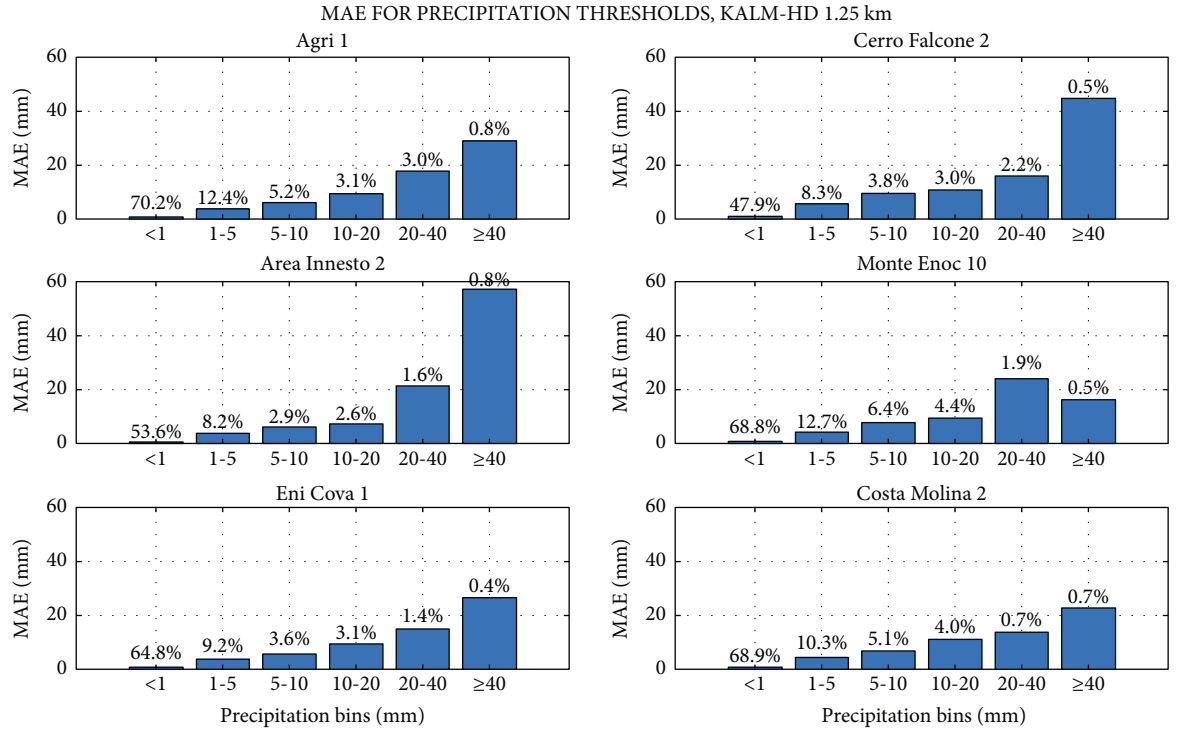

Figure 10: Mean absolute errors for precipitation thresholds in the two years of the observation period over the six weather stations at day +1 as lead time for the KALM-HD model with 1.25 km. Values in red are referred to as the percentage of analyzed events in each bin.

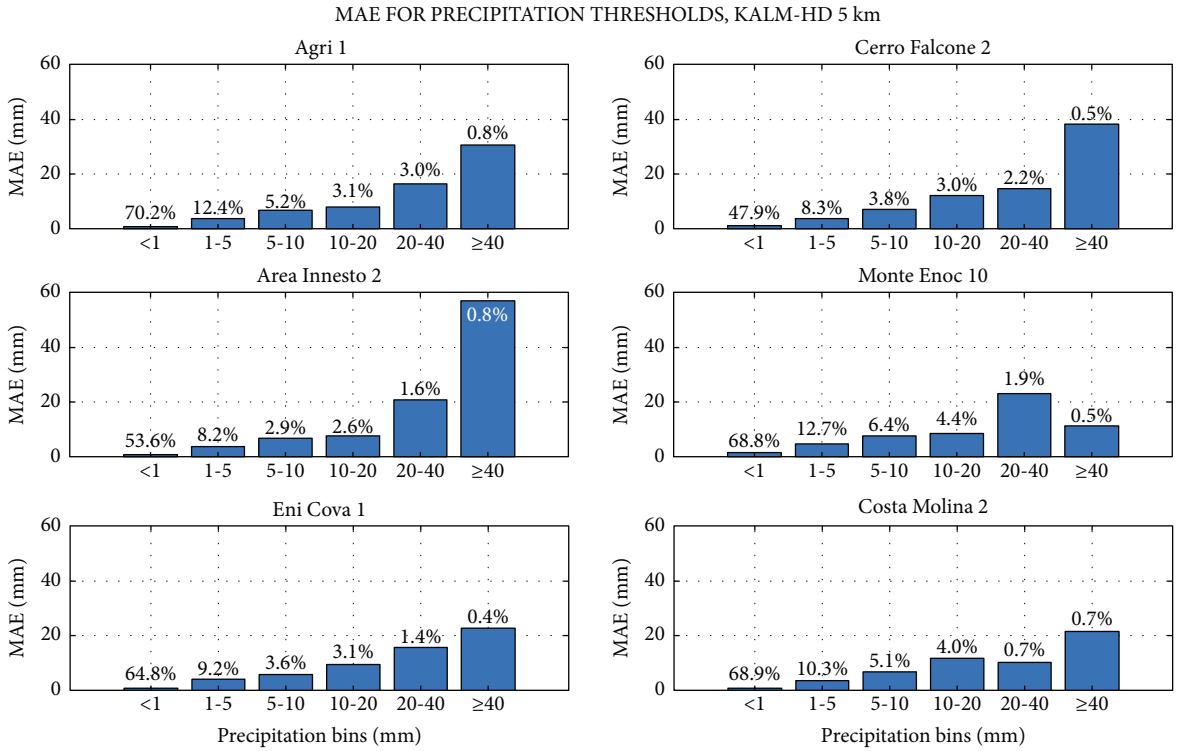

Figure 11: Mean absolute errors for precipitation thresholds in the two years of the observation period over the six weather stations at day +1 as lead time for the KALM-HD model with 5 km. Values in red are referred to as the percentage of analyzed events in each bin.

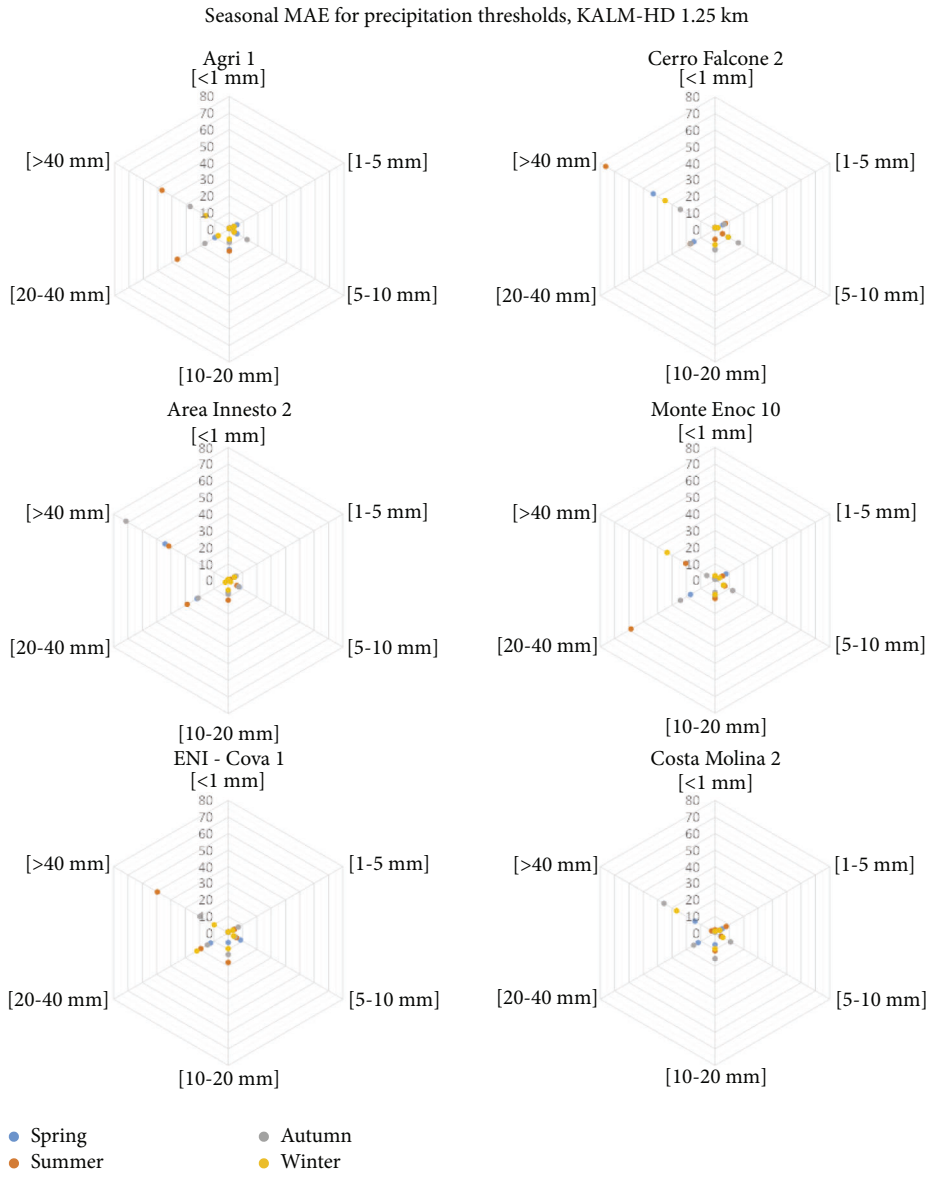

Figure 12: Seasonal MAE for precipitation thresholds in the two years of the observation period over the six weather stations at day +1 as lead time for the KALM-HD model with 1.25 km.

thermal cycles, the temperature prediction in the valley stations can be improved by post-processing forecast data, calibrated by local observations. This can be made by using, for example, a Kalman Filter [53] for discrete time points in a space-state model, which has shown to be extremely effective and computationally efficient. Preliminary analyses, not shown here, have given a significant improvement in terms of skill scores in the valley stations (e.g., the MAE drops below the 2°C thresholds), while only a little or nearly no improvements have been obtained in mountain stations. As expected, spring and autumn have shown some intermediate characteristics between summer and winter, and they will not be shown here for the sake of brevity.

4.1.2. Precipitation Analysis. As for temperatures, precipitation forecasts are scaled on the points where the weather stations are located and aggregated at daily scale. The results generally depict a very similar behavior for the KALM-HD model with the two grid resolutions, although a slightly better performance has been found for the coarser one. This can be explained by considering an excess of drizzle or light rain events associated with the model overestimation of convection at 1.25 km which has not been found in the smoother grid at 5 km. Figures 10 and 11 clearly show how the MAE grows as daily precipitation thresholds increase. Most of the analyzed data are in the first bin (<1 mm) which also includes those days with no (forecasted/observed)

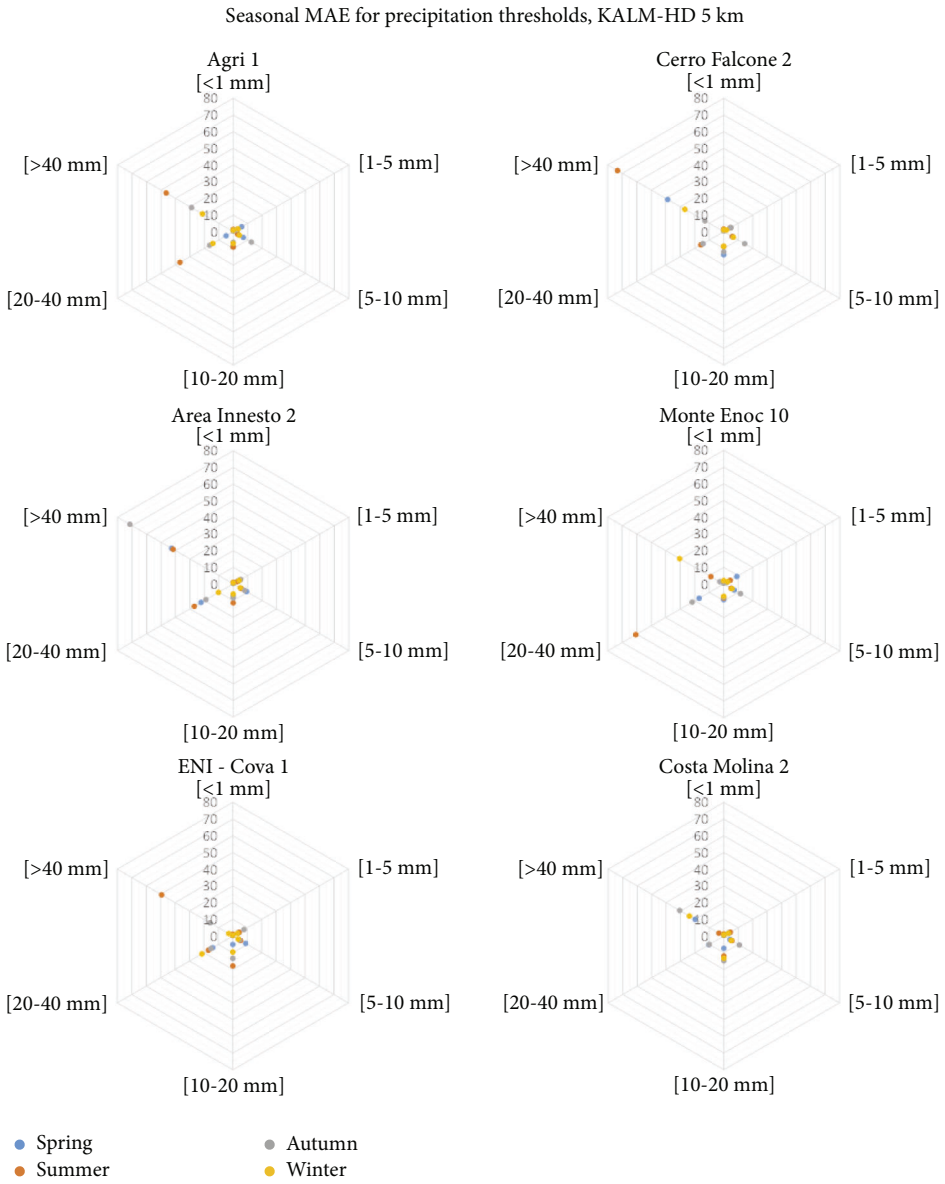

FIGURE 13: Seasonal MAE for precipitation thresholds in the two years of the observation period over the six weather stations at day +1 as lead time for the KALM-HD model with 5 km.

precipitation. On the contrary, a very small percentage (<1%) of severe events has occurred in the two investigated years with high rainfall values still a challenge to be predicted; in fact, thresholds greater than 40 mm show mean absolute errors higher than 30 mm with both resolutions of the KALM-HD model. No significant differences are here noticed about valley and mountain stations in terms of MAE, albeit a very slight worsening of the performance can be found over valley weather stations, where the KALM-HD model appears less able to predict some unstable conditions; this latter characteristic may be quite typical over regions with pronounced orography. The intrinsically limited predictability of the small scales, including convection, requires not only the use of ensembles to generate probabilistic forecasts and assess their confidence [54, 55], but those ensembles require refined initial conditions, which can be obtained by the data assimilation of spatially dense observations [56]. It has been shown [57] that enKF assimilation of radar data may have led to increased forecast skill, but, for the application in Val d'Agri, radar data poorly cover the highest resolution domain, and they cannot be used in the data assimilation of the model. Another impact may come from the latent heat nudging, which has not been implemented here, due to its influence on deep convection.

Looking at the seasonal behavior, greater values of MAE are once again found for higher rainfall thresholds, particularly in summer and autumn seasons for both grid resolutions of the KALM-HD model (Figures 12 and 13), while wintertime shows a lower number of precipitation errors in each threshold bin, which is in agreement with the local rainfall regimes. No relevant seasonal differences are found among stations, according to the main dependence of precipitation by

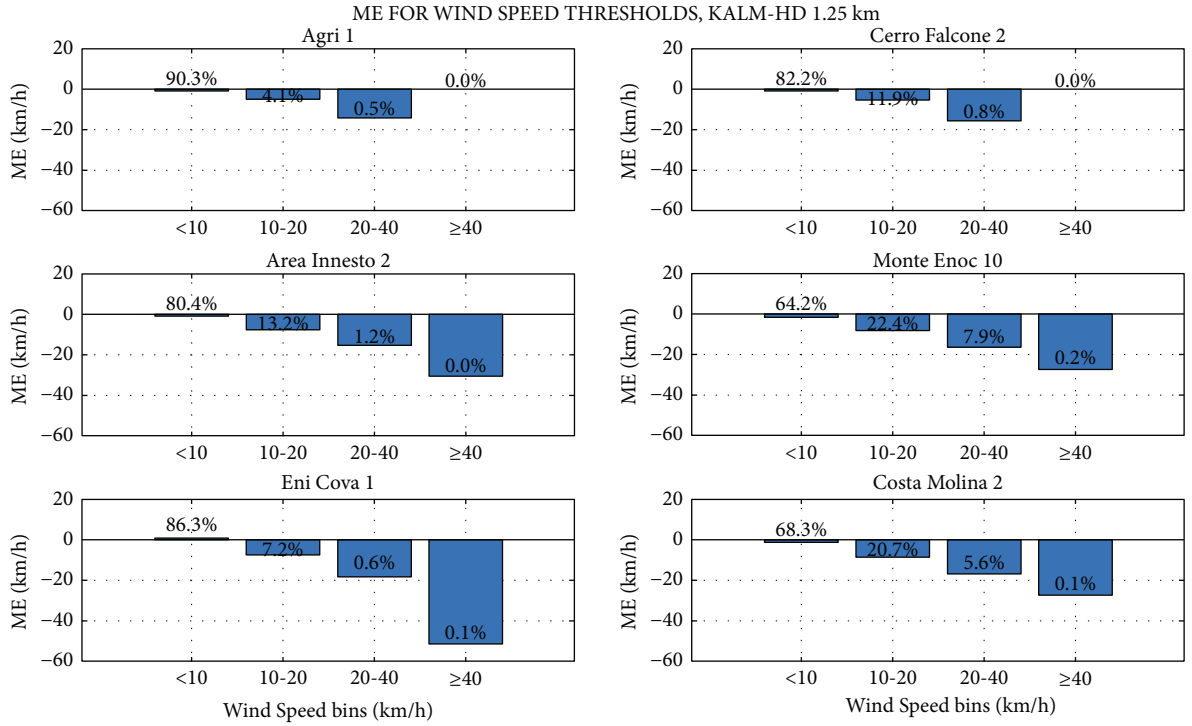

FIGURE 14: Mean errors for wind speed thresholds in the two years of the observation period over the six weather stations at day +1 as lead time for the KALM-HD model with 1.25 km. Values in red are referred to as the percentage of analyzed events in each bin.

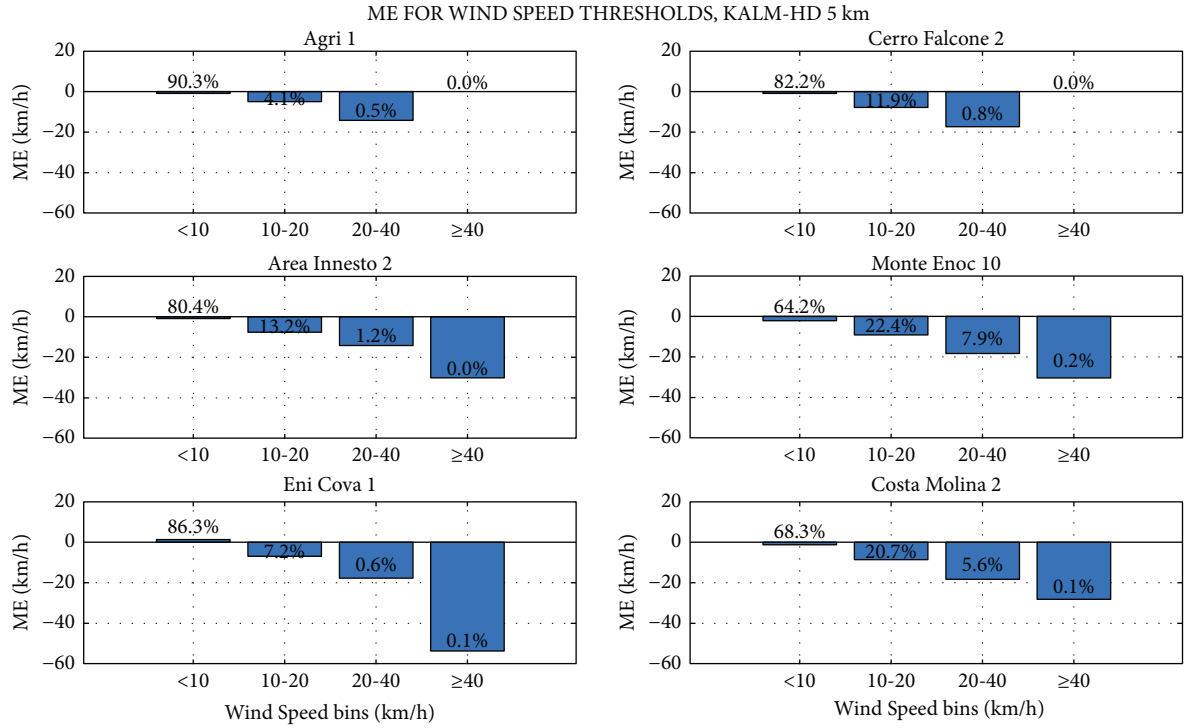

FIGURE 15: Mean errors for wind speed thresholds in the two years of the observation period over the six weather stations at day +1 as lead time for the KALM-HD model with 5 km. Values in red are referred to as the percentage of analyzed events in each bin.

synoptic or mesoscale fluxes, and only marginally by very local conditions, maybe with some exceptions for severe events. However, as noted before, this latter element is probably linked to some limitations of the KALM-HD model to well predict locally induced unstable conditions, which are less relevant in winter than in the other three seasons.

4.1.3. Wind Analysis. The third considered meteorological variable is wind speed, which may be important under several aspects, but, in our context, it has a significant impact on the vegetation of this typical forestry area during the passage of severe storms. Hence, its mechanical action can destabilize the soil increasing the risk of debris flows and slope instability. In this study, thresholds have been conventionally subdivided taking into account those wind velocities which allow generating of energy production, as many wind farms have been installed by the ENI company in the surrounding area of study. Usually, wind speeds below 10 km/h cannot be utilized for wind power, otherwise, values between 10 km/h and 40 km/h are useful for energy production, while intensities above 40 km/h are considered critical conditions.

As for temperatures, results depict a better performance for the model with the highest resolution, comparing measurements with forecasts over the six weather stations. In Figures 14 and 15, a deeper investigation of the ME for wind forecasts is shown using both the model grids. As depicted in the figures, the ME is small, i.e., a good agreement between the model forecast and observed weather data, for low wind velocities which are the majority of analyzed cases. However, as for precipitation, increasing the wind speed threshold, the ME tends to grow. Clearly, it is worthwhile to mention that the KALM-HD has a general tendency to underestimate observed values over all six weather stations. This may be connected to the capability of the model to describe wind regimes in this terrain where the local topography represents a very complex and variable geometry. In fact, a systematic change of valley depth, width, and length induces differences in the cross- and along-valley flow field and thermal structure of the boundary layer, as we above noted discussing the analysis of temperatures. The deeper the valley, the stronger the up-valley winds, and more favored are the formation of vertically stacked circulation cells and an elevated valley inversion layer. Even if this latter characteristic cannot be verified in the Val d'Agri basin, due to a lack of observed vertical profiles and considering all available data including topography, this elevated inversion layer often seems disturbed by the interaction between mesoscale circulation and local thermally driven winds. Only, at Eni Cova station, a slight overestimation is found for low wind regimes in all seasons, due to its position at the bottom of the slope and the presence of drainage flows by a very small north-south oriented valley, not resolved by the model, which may reduce the real wind speeds at that place.

This general underestimation of wind speed forecasts over the six weather stations is confirmed even at seasonal behavior (not shown here for the sake of brevity). This may depend on different causes: in winter and summer, this can be due to an insufficient estimation of upslope and downslope regimes due to the topographic features, among other effects, while in autumn and spring it can be due to the interaction of fluxes at sub-synoptic and mesoscale with local circulation induced by orography and thermal characteristics. As noted for temperature, the forecast error is generally less pronounced for mountain stations, mostly affected by the interaction of synoptic patterns, which are generally more predictable.

5. Conclusions

In the framework of an EWS, essential data come from a weather forecast model to be run at the local scale. The KALM-HD model, based on a local ensemble prediction system, has been applied to investigate the forecast performance in the Val d'Agri area, Basilicata region, in Southern Italy: an Apennine territory affected by several landslides and floods due to its geological characteristics and the dynamics of rainfalls.

This study has concerned with the comparison between two-year hourly and daily predicted and observed data, from December 1st, 2018, to November 30th, 2020, at day +1 as a lead time of forecast in six places, where weather stations are installed and forecast values are scaled to these points.

The benchmark analysis is made by using different skill scores and considering two different model horizontal resolutions: 1.25 km and 5 km.

Results show how the best scores are achieved for the 1.25 km horizontal resolution model in comparison with the 5 km one, concerning temperature and wind forecasts, mostly affected by the interaction of synoptic patterns, which are generally more predictable, while an overestimation in drizzle or light precipitation events slightly worse the performance at 1.25 km.

In regards to temperature data, high scores are achieved for the mountain stations, where valleys' thermal conditions have little influence. On the contrary, in the valley stations, it may be necessary the application of a filtering method to improve the forecast of this variable, especially in winter (DJF), when local subsidence plays an important role. Concerning precipitation, no relevant seasonal differences are found between valley and mountain stations as forecast errors: this is in agreement with the dependence of precipitations mainly by synoptic and mesoscale fluxes, and only marginally by very local conditions with some exceptions in summer (JJA) and autumn (SON) for intense events. Regarding wind speed, which is more difficult to forecast over bottom points of closed valleys, mountain points show lower deviation from observed values than the valley ones, and a general underestimation is present in all seasons and nearly in all stations, except at Eni Cova station where forecasts slightly overestimate low wind speeds.

In conclusion, the KALM-HD short-term forecast uncertainties are quantified with respect to in situ measurements. By increasing the grid spacing from 5 km to 1.25 km, generally, the KALM-HD better represents the reference observations in complex terrain. We believe that KALM-HD has the potential to serve as an input model for forcing parameters needed by the EWS, and we will further investigate the such application. EWS can be easily applied to other areas of interest where critical infrastructures (not only pipelines) can be monitored preventing or mitigating possible hydrogeological risks. In fact, the same approach has now been implemented in the SecureGas project, in the framework of the European Horizon 2020, which aims at

securing the European Gas Network from cyberphysical threats. In this latter project, forecast data from the KALM-HD model are provided for a large region covering the North-West of Italy [58]. Once again, the meteorological forecasts and observations are a necessary input to the geohazard modeling system, which triggers early warnings in case of risk in rainfall-induced landslides. This other application has taken advantage of the knowledge and experience of what has been developed for the Val d'Agri area, demonstrating its capability to be generally extended where critical infrastructures may be threatened by weather-related geohazards.

Data Availability

The meteorological data used to support the findings of this study are available from the corresponding author upon request.

Conflicts of Interest

The authors declare that they have no conflicts of interest.

Acknowledgments

The present work has been developed under the framework of the project on the Early Warning System for Hydro and Pollution Risks, carried out by Eni S.p.A. The authors would like to thank Dr. Dario Avagliano, Alice Pozzoli, Antonella Caputi, and Michele Tricarico for their on-field support and maintenance service in the Val d'Agri during the last three years. Lastly, the authors also thank Eng. Nicolás Chaves González for his graphical support.

References

[1] P. Ni, S. Mangalathu, and Y. Yi, "Fragility analysis of continuous pipelines subjected to transverse permanent ground deformation," *Soils and Foundations*, vol. 58, no. 6, pp. 1400–1413, 2018.

[2] V. Marinos, G. Stoumpos, and C. Papazachos, "Landslide hazard and risk assessment for a natural gas pipeline project: the case of the trans adriatic pipeline, Albania section," *Geosciences*, vol. 9, no. 2, 2019.

[3] F. Guzzetti, S. Peruccacci, M. Rossi, and C. P. Stark, "Rainfall thresholds for the initiation of landslides in central and southern Europe," *Meteorology and Atmospheric Physics*, vol. 98, no. 3-4, pp. 239–267, 2007.

[4] L. Olivares, E. Damiano, P. Mercogliano et al., "A simulation chain for early prediction of rainfall-induced land-slides," *Landslides*, vol. 11, no. 5, pp. 765–777, 2014.

[5] A. Abbate, M. Papini, and L. Longoni, "Analysis of meteorological parameters triggering rainfall-induced landslide: a review of 70 years in Valtellina," *Natural Hazards and Earth System Sciences*, vol. 21, no. 7, pp. 2041–2058, 2021.

[6] M Reinsurance Company (Munich Re), "Topics geo natural catastrophes," *Analyses, Assessments, Positions*, Munich Re, München, Germany, 2016.

[7] J. N. Brown and B. M. Peake, "Sources of heavy metals and polycyclic aromatic hydrocarbons in urban stormwater runoff," *Science of the Total Environment*, vol. 359, no. 1–3, pp. 145–155, 2006.

[8] A. M. Cruz and E. Krausmann, "Vulnerability of the oil and gas sector to climate change and extreme weather events," *Climatic Change*, vol. 121, no. 1, pp. 41–53, 2013.

[9] S. A. Karamanos, A. M. Gresnigt, and G. J. Dijkstra, *Geohazards and Pipelines: State-Of-The-Art Design Using Experimental, Numerical and Analytical Methodologies*, Book Springer Nature, Berlin, Germany, 2020.

[10] "EGIG 11th Report," 2020, https://www.egig.eu/reports.

[11] M. J. Crozier, "Deciphering the effect of climate change on landslide activity: a review," *Geomorphology*, vol. 124, no. 3-4, pp. 260–267, 2010.

[12] S. L. Gariano, G. Rianna, O. Petrucci, and F. Guzzetti, "Assessing future changes in the occurrence of rainfall-induced landslides at a regional scale," *Science of the Total Environment*, vol. 596-597, pp. 417–426, 2017.

[13] F. Ciervo, G. Rianna, P. Mercogliano, and M. N. Papa, "Effects of climate change on shallow landslides in a small coastal catchment in southern Italy," *Landslides*, vol. 14, no. 3, pp. 1043–1055, 2017.

[14] S. L. Gariano and F. Guzzetti, "Landslides in a changing climate," *Earth-Science Reviews*, vol. 162, pp. 227–252, 2016.

[15] E. Canli, B. Loigge, and T. Glade, "Spatially distributed rainfall information and its potential for regional landslide early warning systems," *Natural Hazards*, vol. 103, 2017.

[16] B. Thiebes, S. Bai, Y. Xi, T. Glade, and R. Bell, "Combining landslide susceptibility maps and rainfall thresholds using a matrix approach," *Revista De Geomorfologie*, vol. 19, 2017.

[17] E. Canli, M. Mergili, B. Thiebes, and T. Glade, "Probabilistic landslide ensemble prediction systems: lessons to be learned from hydrology," *Natural Hazards and Earth System Sciences*, vol. 18, no. 8, pp. 2183–2202, 2018.

[18] G. Devoli, I. Kleivane, M. Sund, N. Orthe, R. Ekker, and E. Johnsen, "Landslide early warning system and web tools for real-time scenarios and for distribution of warning messages in Norway," in *Proceedings of the Engineering Geology for Society and Territory*, vol. 2, pp. 625–629, Springer, Berlin, Germany, 2015.

[19] G. Devoli, D. Tiranti, R. Cremonini, M. Sund, and S. Boje, "Comparison of landslide forecasting services in piedmont (Italy) and Norway, illustrated by events in late spring 2013," *Natural Hazards and Earth System Sciences*, vol. 18, no. 5, pp. 1351–1372, 2018.

[20] SECUREGAS-Securing European Gas Network, "Project H2020-SU-INFRA01, grant agreement n. 833017, deliverable report D6.1: business case 3 scenario definition-main document," 2020, https://www.securegas-project.eu.

[21] "HORIZON 2020 SecureGas project website," 2020, https://www.securegas-project.eu/.

[22] S. Segoni, G. Rossi, A. Rosi, and F. Catani, "Landslides triggered by rainfall: a semi-automated procedure to define consistent intensity–duration thresholds," *Computers & Geosciences*, vol. 63, pp. 123–131, 2014.

[23] S. Peruccacci, M. T. Brunetti, S. L. Gariano, M. Melillo, M. Rossi, and F. Guzzetti, "Rainfall thresholds for possible landslide occurrence in Italy," *Geomorphology*, vol. 290, pp. 39–57, 2017.

[24] G. Giunta, R. Salerno, A. Ceppi, G. Ercolani, and M. Mancini, "Benchmark analysis of forecasted seasonal temperature over different climatic areas," *Geoscience Letters*, vol. 2, no. 1, p. 9, 2015.

[25] M. Piccarreta, A. Pasini, D. Capolongo, and M. Lazzari, "Changes in daily precipitation extremes in the Mediterranean from 1951 to 2010: the Basilicata region, southern Italy,"

International Journal of Climatology, vol. 33, no. 15, pp. 3229–3248, 2013.

[26] F. T. Gizzi, M. Proto, and M. R. Potenza, "The Basilicata region (Southern Italy): a natural and "human-built" open-air laboratory for manifold studies. Research trends over the last 24 years (1994–2017)," *Geomatics, Natural Hazards and Risk*, vol. 10, no. 1, pp. 433–464, 2019.

[27] M. L. Clarke and H. M. Rendell, "Hindcasting extreme events: the occurrence and expression of damaging floods and landslides in southern Italy," *Land Degradation & Development*, vol. 17, no. 4, pp. 365–380, 2006.

[28] C. Di Maio, R. Vassallo, M. Vallario, S. Pascale, and F. Sdao, "Structure and kinematics of a landslide in a complex clayey formation of the Italian southern Apennines," *Engineering Geology*, vol. 116, no. 3-4, pp. 311–322, 2010.

[29] M. Lazzari, *Note Illustrative Della Carta Inventario Delle Frane Della Basilicata Centroccidentale*, Editore Zaccara, Lagonegro, Italy, 2011.

[30] M. Piccarreta, D. Capolongo, F. Boenzi, and M. Bentivenga, "Implications of decadal changes in precipitation and land use policy to soil erosion in Basilicata, Italy," *Catena*, vol. 65, no. 2, pp. 138–151, 2006.

[31] S. F. Dal Sasso, S. Manfreda, G. Capparelli et al., "Hydrological and geological hazards in Basilicata," *L'Acqua*, vol. 3, pp. 77–85, 2017.

[32] T. Caloiero, A. A. Pasqua, and O. Petrucci, "Damaging hydrogeological events: a procedure for the assessment of severity levels and an application to Calabria (southern Italy)," *Water*, vol. 6, no. 12, pp. 3652–3670, 2014.

[33] L. Aceto, T. Caloiero, A. A. Pasqua, and O. Petrucci, "Analysis of damaging hydrogeological events in a Mediterranean region (Calabria)," *Journal of Hydrology*, vol. 541, pp. 510–522, 2016.

[34] G. Giunta, R. Salerno, A. Ceppi, G. Ercolani, and M. Mancini, "Effects of model horizontal grid resolution on short- and medium-term daily temperature forecasts for energy consumption application in European cities," *Advances in Meteorology*, vol. 2019, Article ID 1561697, 12 pages, 2019.

[35] D. S. Wilks, *Statistical Methods in the Atmospheric Sciences*, Academic Press, Elsevier, Amsterdam, Netherlands, 2nd edition, 2006.

[36] I. T. Jolliffe and D. B. Stephenson, *Forecast Verification: A Practitioner's Guide in Atmospheric Science*, John Wiley & Sons, Hoboken, NJ, USA, 2003.

[37] "WWRP/WGNE Joint Working Group on Verification," 2003, https://www.cawcr.gov.au/projects/verification.

[38] G. Giunta, R. Vernazza, R. Salerno, A. Ceppi, G. Ercolani, and M. Mancini, "Hourly weather forecasts for gas turbine power generation," *Meteorologische Zeitschrift*, vol. 26, no. 3, pp. 307–317, 2017.

[39] G. Giunta and R. Salerno, "Short to long term meteorological forecasting system for the production, management and sale of energy resources," Patent PCT/IB2013/054780, 2015.

[40] W. A. Lahoz and P. Schneider, "Data assimilation: making sense of earth observation," *Frontiers in Environmental Science*, vol. 2, 2014.

[41] P. L. Houtekamer and H. L. Mitchell, "Data assimilation using an ensemble Kalman filter technique," *Monthly Weather Review*, vol. 126, no. 3, pp. 796–811, 1998.

[42] J. P. Hacker and C. Snyder, "Ensemble Kalman filter assimilation of fixed screen-height observations in a parameterized PBL," *Monthly Weather Review*, vol. 133, no. 11, pp. 3260–3275, 2005.

[43] T. Fujita, D. J. Stensrud, and D. C. Dowell, "Surface data assimilation using an ensemble Kalman filter approach with initial condition and model physics uncertainties," *Monthly Weather Review*, vol. 135, no. 5, pp. 1846–1868, 2007.

[44] Z. Meng and F. Zhang, "Tests of an ensemble Kalman filter for mesoscale and regional-scale data assimilation. Part III: comparison with 3DVAR in a real-data case study," *Monthly Weather Review*, vol. 136, no. 2, pp. 522–540, 2008.

[45] S. Y. Ha and C. Snyder, "Influence of surface observations in mesoscale data assimilation using an ensemble kalman filter," *Monthly Weather Review*, vol. 142, no. 4, pp. 1489–1508, 2014.

[46] S. Dirren, R. D. Torn, and G. J. Hakim, "A data assimilation case study using a limited-area ensemble Kalman filter," *Monthly Weather Review*, vol. 135, no. 4, pp. 1455–1473, 2007.

[47] G. P. Compo, J. S. Whitaker, and P. D. Sardeshmukh, "Feasibility of a 100-year reanalysis using only surface pressure data," *Bulletin America Meteorology Social*, vol. 87, no. 2, pp. 175–190, 2006.

[48] J. L. Anderson, "Spatially and temporally varying adaptive covariance inflation for ensemble filters," *Tellus*, vol. 61, no. 1, pp. 72–83, 2009.

[49] J. P. Hacker, S. Y. Ha, C. Snyder et al., "The U.S. air force weather agency's mesoscale ensemble: scientific description and performance results," *Tellus A: Dynamic Meteorology and Oceanography*, vol. 63, no. 3, pp. 625–641, 2011.

[50] J. Berner, S. Y. Ha, J. P. Hacker, A. Fournier, and C. Snyder, "Model uncertainty in a mesoscale ensemble prediction system: stochastic versus multiphysics representations," *Monthly Weather Review*, vol. 139, no. 6, pp. 1972–1995, 2011.

[51] I. Orlanski, "A rational subdivision of scales for atmospheric processes," *Bulletin of the American Meteorological Society*, vol. 56, no. 5, pp. 527–530, 1975.

[52] R. B. Stull, *An Introduction to Boundary Layer Meteorology*, Springer, Berlin, Germany, 1988.

[53] R. E. Kalman, "A new approach to linear filtering and prediction problems," *Journal of Basic Engineering*, vol. 82, no. 1, pp. 35–45, 1960.

[54] E. N. Lorenz, "The predictability of a flow which possesses many scales of motion," *Tellus*, vol. 21, no. 3, pp. 289–307, 1969.

[55] J. Slingo and T. Palmer, "Uncertainty in weather and climate prediction," *Philosophical Transactions of the Royal Society A: Mathematical, Physical & Engineering Sciences*, vol. 369, no. 1956, pp. 4751–4767, 2011.

[56] A. Johnson and X. Wang, "A study of multiscale initial condition perturbation methods for convection-permitting ensemble forecasts," *Monthly Weather Review*, vol. 144, no. 7, pp. 2579–2604, 2016.

[57] K. Bachmann, C. Keil, G. C. Craig, M. Weissmann, and C. A. Welzbacher, "Predictability of deep convection in idealized and operational forecasts: effects of radar data assimilation, orography, and synoptic weather regime," *Monthly Weather Review*, vol. 148, no. 1, pp. 63–81, 2020.

[58] F. Ioele, C. Evangelista, G. Malgesini et al., "Rainfall-induced landslide forecast tool: an application to gas pipelines," in *Proceedings of the 3rd International Conference on Natural Hazards & Infrastructure*, ICONHIC, Athens, Greece, July 2022.